Available online at www.sciencedirect.com
SCIENCE DIRECT®
Nuclear Instruments and Methods in Physics Research A 536 (2005) 136–145
NUCLEAR INSTRUMENTS & METHODS IN PHYSICS RESEARCH Section A
www.elsevier.com/locate/nima

BGO readout with photodiodes as a soft gamma-ray detector at −30 °C ☆

T. Nakamoto[a], Y. Fukazawa[a,*], T. Ohsugi[a], T. Kamae[b], J. Kataoka[c]

[a]*Department of Physical Sciences, Hiroshima University, 1-3-1 Kagamiyama, Higashi-Hiroshima, Hiroshima 739-8526, Japan*
[b]*Stanford Linear Accelerator Center, Menlo Park, CA, USA*
[c]*Tokyo Institute of Technology, Tokyo, Japan*

Received 5 April 2004; accepted 9 July 2004
Available online 19 August 2004

Abstract

BGO is expected to be plausible devices for soft gamma-ray detectors, because of a high detection efficiency for soft gamma-rays. Here we report on the good performance of BGO readout with PIN—photodiode or avalanche photodiode as a soft gamma-ray detector. We confirmed that the signal output of BGO becomes comparable to that of GSO when it is readout with photodiodes due to better matching between emission wavelength of BGO and quantum efficiency of photodiode. The energy resolution of 6.2% and 3.4% for 662 and 1836 keV, respectively, gamma-rays at −30 °C is obtained with the combination of the $5 \times 5 \times 5\,mm^3$ cube BGO and the Hamamatsu avalanche photodiode (APD) S8664-55. In this combination, the lowest detectable energy is found to be ~ 10 keV. These performances are better than that obtained with Photomultiplier tube (PMT), and our results increase many possible applications of BGO readout with photodiodes as soft gamma-ray detectors.

PACS: 07.85. – m; 07.85.Nc; 95.55.Ka

Keywords: BGO scintillator; Photodiode; Avalanche photodiode; Gamma-ray detector

1. Introduction

Bismuth Germanate $Bi_4Ge_3O_{12}$ (BGO) crystal scintillator has gathered attention in terms of its high stopping power for soft gamma-rays (Table 1). Therefore, BGO enables us to construct a detector with lower weight, which are essential for the developments of gamma-ray detector in

☆The authors are grateful to T. Itoh (Baikowski Japan Co.) for supplying and cutting BGO scintillators of high quality. This work is carried out as a part of "Ground-based Research Announcement for Space Utilization" promoted by Japan Space Forum.

*Corresponding author. Tel.: +81-82-424-7380; fax: +81-82-424-0727.
E-mail address: fukazawa@hirax6.hepl.hiroshima-u.ac.jp (Y. Fukazawa).

0168-9002/$ - see front matter © 2004 Elsevier B.V. All rights reserved.
doi:10.1016/j.nima.2004.07.209

Table 1
Comparison of major inorganic scintillators

Scintillator	NaI:Tl	CsI:Tl	GSO	BGO
Effective atomic number	50	54	59	74
Density (g/cm^3)	3.67	4.51	6.71	7.13
Peak wavelength (nm)	410	565	430	480
Light yield (relative)	100	45	20	12
Scintillation time (ns)	230	1000	60	300
Mean free path (511 keV:cm^{-1})	0.34	0.41	0.674	0.955

space. Non-deliquescence and good light-output linearity of BGO are also advantageous. However, its scintillation light yield is known to be only $\sim$ 10–15% of NaI. Alternatively, Gd_2SiO_5(Ce) (GSO) scintillators which have a higher light yield, 40% of NaI [1], are often used as a main sensor since GSO has a somewhat smaller effective atomic number than BGO but higher than low-Z popular crystals such as NaI or CsI. BGO has been primarily used as an active shield, because a large volume of a single BGO crystal is available. For example, a phoswich counter consisting of GSO and BGO are applied in the astrophysical soft gamma-ray detector onboard the Astro-E2 satellite [2,3].

For soft gamma-ray detection, BGO is usually readout by the photo-multiplier tube (PMT) because of its low light yield. The peak wavelength of BGO scintillation light is around 480 nm, and it does not match well the PMT-sensitive peak around 400 nm. PMT has a low quantum efficiency of at most 20–25% even at the peak sensitivity, and thus a large portion of BGO scintillation light is thought to be lost. On the other hand, Silicon PIN Photodiode (PD) has a high quantum efficiency of $\sim$ 80% above $>$400 nm, but a small signal output of PD combined with scintillators limited the application due to low signal-to-noise (S/N) ratio. The combination of CsI + PD is known to be a good combination because longer wavelength and higher light yield of CsI scintillation helps to generate high signal output and improve S/N ratio of PD signal. The low signal-to-noise ratio of photodiodes is thought to be compensated by avalanche photodiodes (APD), where the signal is amplified by avalanche with a gain of 10–100. However, for a long time, a small entrance window and a large dark current of APD have hindered the readout of scintillators for soft gamma-rays.

Recently, improved silicon-process technology enables us to use PD and APD with low noise and large size for soft gamma-ray detectors combined with scintillators. For example, Kamae et al. [1] showed that the GSO readout with PD gives energy resolution comparable to or better than the NaI(Tl). Good performance of large-area avalanche photodiodes is also reported by Moszyński et al. (e.g. Ref. [4]) and Ikagawa et al. [5] for APDs produced by Advanced Photonix, Inc. (API) and Hamamatsu Photonics (HPK), respectively. Moszyński et al. [6] reported a good energy resolution of 5.8% at 662 keV for BGO readout with APD at about 100 K. This is mainly due to 3 times larger light output of BGO than at room temperature.

Following these results, BGO scintillator readout with photodiodes becomes a possible excellent detector of soft gamma-rays at a mildly cooled environment, such as cosmic gamma-ray detectors onboard the satellite. Below a gamma-ray energy of 500 keV, CdTe and CdZnTe semi-conductor devices have become a good candidate of detectors because of its superior energy resolution (e.g. Ref. [7]), while BGO is still necessary for detection of higher-energy gamma-rays or active shield. Previous studies on the BGO scintillator reported that the number of photoelectrons in the PMT and PD is 980 MeV^{-1} and 4750–5300 MeV^{-1}, respectively, at the room temperature [8]. These values are very small compared with 3840 MeV^{-1} and 37000 MeV^{-1} of CsI. The energy resolution of BGO in Moszyński et al. [10] is 10.2% and 7.8% at 662 keV for the readout with PMT and APD, respectively. However, PMT energy resolution of

10.2% is too bad for the size of $\phi 9 \times 9$ in mm; even a large size BGO for the Astro-E2 Hard X-ray detector with a size of $\sim 60 \times 60 \times 60$ mm gives an energy resolution of $\sim 10\%$ at 662 keV (Hard X-ray Detector (HXD) team internal report.) Therefore, their BGO crystal may be of low quality. It should be noticed that, at lower temperature, dark current of photodiodes becomes lower and BGO light yield increases, while that of CsI decreases. This indicates that a combination of BGO and photodiodes at the lower temperature is expected to show a much better performance. Here, we report the excellent performance of BGO readout with PD and APD as a soft gamma-ray detector at $-30\,^{\circ}$C.

2. BGO crystals and photodiodes

BGO crystals used here was supplied by Crismatec Company. The specification of delivery is in such a way that the light output readout with PMT is 10–15% of NaI at room temperature, and light transmission length is as long as 350–400 cm at 450 nm. Such a good light transparency is important to use BGO as a long-plate active shield, for example, as in the Astro-E2 (HXD). Here we tested a small-size BGO cube of $5 \times 5 \times 5\,\mathrm{mm}^3$, in order to evaluate the performance of BGO and photodiode combination. For comparison, we also measured CsI and GSO of the same size as the BGO cube.

For PD, we employed the Hamamatsu SPL-PD-type A ($5 \times 5\,\mathrm{mm}^2$ area) which experimentally was made to extend the light sensitivity toward the shorter wavelength for the blue-light of GSO scintillation [1]. In addition, we tested the Hamamatsu S8664-55 ($5 \times 5\,\mathrm{mm}^2$ area) for APD. The detailed properties of S8664-55 are reported by Ikagawa et al. [5], and a body capacitance and a dark current are improved by the buried-junction structure. Entrance window of both photodiodes is coated for protection. We checked the body-capacitance and leakage current of our PD and APD at room temperature as shown in Fig. 1. The full depletion voltage is around 20 V and 300–350 V for PD and APD, respectively. Considering this voltage together with the noise performance, we hereafter set the bias voltage to 40 V for PD and 290 V for APD, where the body capacitance is 11.6 pF for PD and 99.2 pF for APD. The reason to choose the above bias voltage of APD is described in Section 5. The leakage current of both APD and PD becomes smaller by two orders of magnitude at $-30\,^{\circ}$C, and thus negligible for the noise performance.

In Fig. 2, the setup diagrams are shown. Measurements were performed at $-30\,^{\circ}$C so that we could ignore the noise associated with the leakage current. The gain of APD is ~ 26 at 290 V and $-30\,^{\circ}$C. Since the CsI light yield decreases with the temperature, we performed the measurements of CsI at room temperature. We tested several layers of white Teflon tape, $BaSO_4$ powder

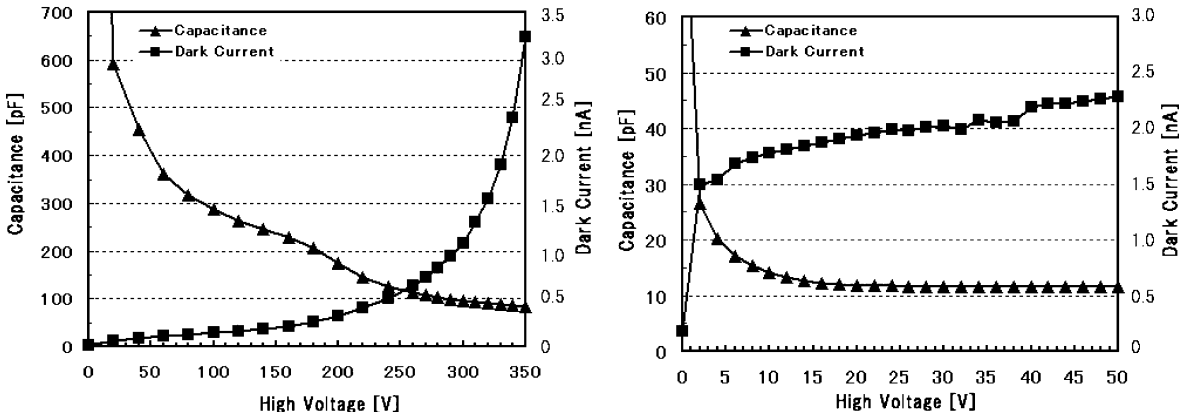

Fig. 1. Body capacitance and leakage current of APD (left) and PD (right), which we presented here, against the bias voltage.

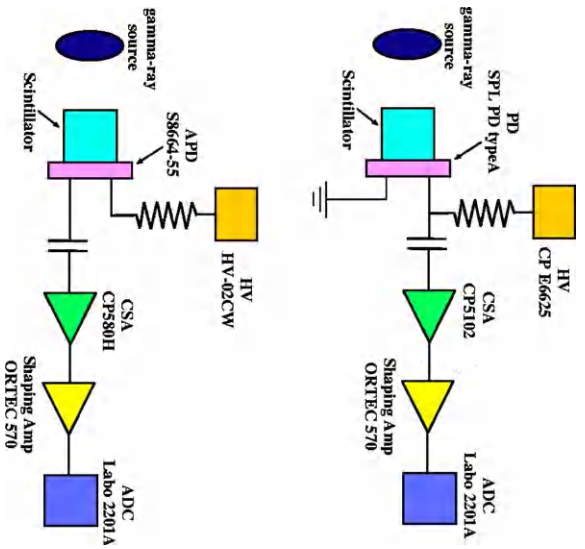

Fig. 2. Setup diagrams of measurements for PD (right) and APD (left).

painted with the glue, and multilayer-polymer mirror VM 2000, as the light reflector of BGO, and chose VM 2000 because of its highest reflectivity. Then, scintillators were wrapped with VM 2000, and coupled to the entrance window of photodiodes directly with the silicone optical grease OKEN 6262A. The bias voltage was supplied via the 50 MΩ load resistor. Hole signals from the P electrode of these photodiodes were input to the AC-coupling low-noise charge sensitive amplifier (ClearPulse CP 580H), and fed into the ADC (Laboratory Equipment Co. AD 2201A) via the shaping amplifier (Ortec 570). The equivalent noise charge attributed to the body-capacitance of photodiode is measured to be $100 \pm 20e^-$ and $310 \pm 30e^-$ for PD and APD, respectively. When we irradiated the gamma-ray directly to the PD, the energy resolution of 1.6 keV at 59.5 keV of the ^{241}Am source was obtained at $-30\,^{\circ}$C.

3. Energy resolution for gamma-rays

The energy resolution $\Delta E/E$ of scintillators coupled with the PMT and photodiode is given as

$$(\Delta E/E)^2 = (\delta_{sc})^2 + 2.355^2 F/N + (\delta_{noise}/N)^2$$

where N is a number of photoelectrons in the PMT or electron-hole pairs in the photodiode, F is the Fano factor or an excess noise factor attributed to the fluctuation of avalanche in the APD, δ_{sc} is an intrinsic energy resolution for the scintillator relevant to the properties of the scintillator itself [9], and δ_{noise} is an electric noise [4]. Generally, the first term is dominant for high energy gamma-rays, the second term is dominant for readout with the PMT, PD, and APD where F is ~ 1, ~ 0.1, and 2–3, respectively, and the last term mainly determined the energy resolution for the readout with PD.

3.1. Readout with PMT

First of all, we measured the energy resolution of scintillators by coupling to the PMT, in order to compare them with those obtained with photodiodes. The Hamamatsu R1847 is used for this measurement. Scintillators were attached on the PMT window with the silicone oil KE108. Since BGO, GSO, and CsI have a $\sim 1\,\mu$s decay component in the scintillation, the shaping time of $<1\,\mu$s significantly loses the signal. Then, the shaping time is chosen to be $2\,\mu$s, since the shaping time of $>2\,\mu$s does not give a better resolution. In Fig. 3, the pulse–height spectra of 662 keV from the ^{137}Cs source were displayed. The relative peak pulse–height and energy resolution at 662 keV are

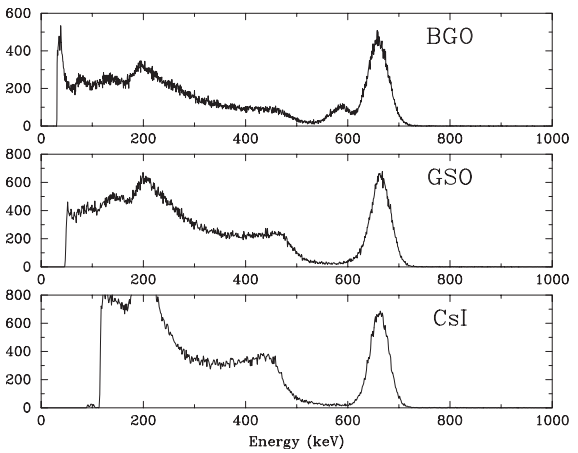

Fig. 3. Pulse–height spectra of ^{137}Cs for scintillators readout with PMT; BGO (top), GSO (middle), CsI (bottom).

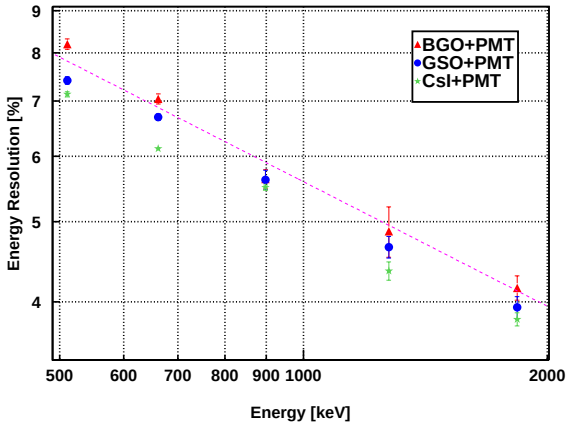

Fig. 4. Energy resolution (FWHM) of scintillators readout with PMT against the gamma-ray energy. The dashed line represents the relation of $\propto E^{-0.5}$.

found to be 1, 1.24 ± 0.02, 1.71 ± 0.03, and $7.0 \pm 0.1\%$, $6.7 \pm 0.1\%$, and $6.1 \pm 0.1\%$ for BGO, GSO, and CsI, respectively. These values indicate that our sample of scintillators exhibit a very good performance; the good energy resolution of 7.0% for BGO + PMT is not yet available in any paper, and 6.7% of GSO is comparable to that in Kamae et al. [1]. In Fig. 4, the energy resolution obtained with various radio-isotopes is plotted against the input gamma-ray energy E. The dependence of $1/\sqrt{E}$ is clearly seen for all the scintillators, indicating that the energy resolution is mainly determined by the Poisson statistics of photoelectrons generated in the PMT.

4. Readout with PD

Next, we measured the performance of scintillators readout with PIN photodiodes. In this experiment, we evaluated not only the energy resolution but also the number of electron–hole pairs.

At first, we investigated the energy resolution against the shaping time, since not only collection of scintillation signals and but also a filter of noise are dependent on the shaping time τ. In Fig. 5, we plotted the pulse–height and energy resolution against τ. Shorter τ gives lower pulse height and worse energy resolution, and they are nearly constant at $\tau > 3\,\mu s$. This is due to the loss of scintillation signals at shorter τ. The loss is the most significant for CsI, and the least for GSO, following their scintillation decay time. Another reason is that, in the case the capacitance noise is dominant as in this measurement, the noise becomes larger at shorter τ. In the following, we set τ to $3\,\mu s$. In Fig. 6, the pulse–height spectra of 662 keV were shown. The relative peak pulse–height becomes $1, 0.99 \pm 0.01$, and 3.5 ± 0.3 for BGO, GSO, and CsI, indicating that the light collection ratio of BGO to GSO becomes 1.25 times as large as that readout with the PMT. This confirmed the prediction described in Section 1; PMT may lose a significant amount of scintillation light of BGO in the photo-electric conversion, and therefore the light yield of BGO is not so low as ever known, but comparable to that of GSO at $-30\,^{\circ}C$.

The energy resolution is plotted in Fig. 7, as a function of incident gamma-ray energy. The relations at the lower energy follows E^{-1}, and their slope becomes milder toward the higher energy, indicating that the noise determines the energy resolution for lower energy gamma-ray, while light photon statistics does for higher energy gamma-ray. However, the slope above 1 MeV is somewhat flatter than the relation of $E^{-0.5}$. This flattening is prominent for CsI, and this is a well-known trend due to the intrinsic energy resolution δ_{sc} of CsI (e.g. Ref. [8]). On the other hand, the energy resolution of CsI becomes similar to BGO and GSO around 1500 keV regardless that it is much better at the lower energy. This is according to the good light-output linearity and low δ_{sc} of BGO and GSO. Therefore, for MeV gamma-rays, the scintillator BGO and GSO will be more useful than CsI because the energy resolution is not so bad than CsI and the stopping power is much higher.

Measuring the pulse–height spectra when low energy gamma-rays such as 31 keV of ^{133}Ba and 59.5 keV of ^{241}Am are absorbed by the PD, we confirmed that the peak pulse–height of PD is 28.8 ± 0.10 times as large as that of BGO + PD signals for the same incident gamma-ray energy. This indicates that the electric noise of 1.6 keV (Si),

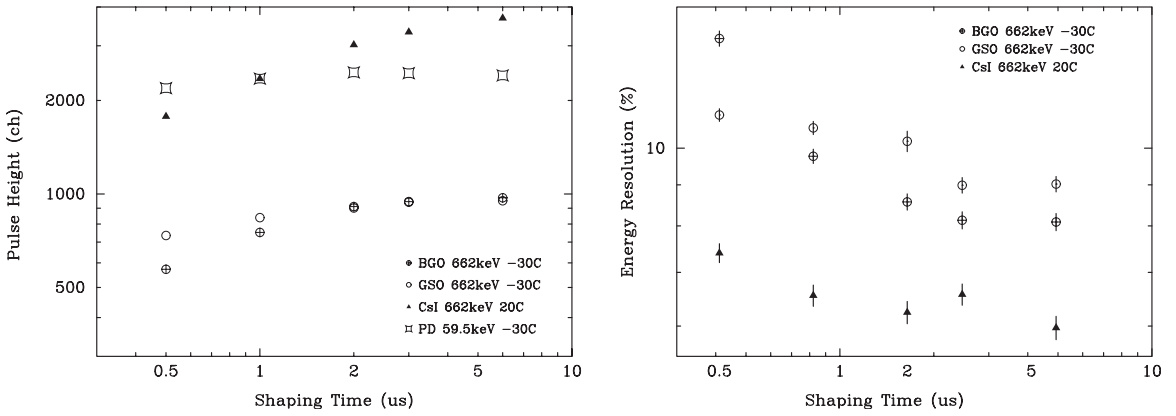

Fig. 5. Pulse–height (left) and energy resolution (right) of ^{137}Cs against the shaping time τ for scintillators readout with PD.

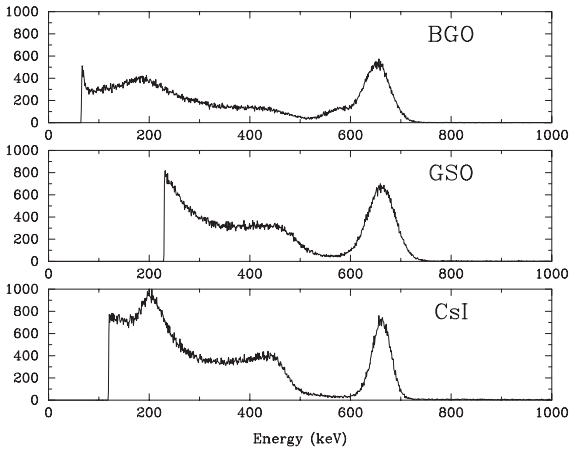

Fig. 6. Pulse–height spectra of ^{137}Cs for scintillators readout with PD; BGO (top), GSO (middle), CsI (bottom).

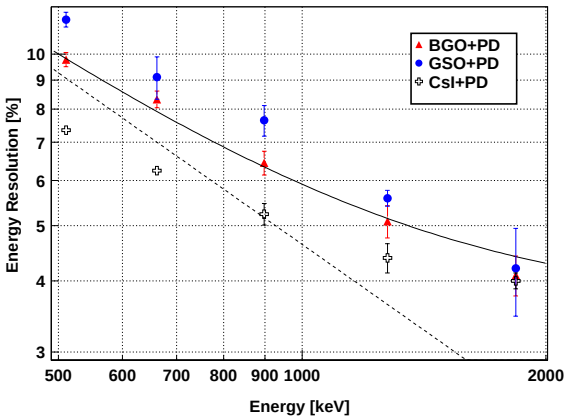

Fig. 7. Energy resolution (FWHM) of scintillators readout with PD against the gamma-ray energy. The dashed line considers the electric noise and Poisson statistics of e–h pairs, and the solid line additionally includes the intrinsic energy resolution (see text in detail).

obtained for gamma-rays detected by PD directly, corresponds to the energy resolution of

$$\delta E_{\text{noise}} = 7.0(E/662\,\text{keV})^{-1}\,\%$$

for BGO + PD (the last term of the equation in Section 2), and the number of electron–hole pairs produced in the BGO + PD is $(9.8 \pm 0.2) \times 10^3$ and $(5.8 \pm 0.2) \times 10^3$ pairs MeV^{-1} at -30° and 20°, respectively. The latter number of pairs is in good agreement with the previous works [11]. Then, the poisson noise of electron–hole pairs (the second term of the equation in Section 2) is estimated to be $\delta E_{\text{Poisson}} = 0.92(E/662\,\text{keV})^{-0.5}\,\%$, where we assume the Fano factor of 0.1. In Fig. 7, we plot the predicted energy resolution of $\delta E = \sqrt{\delta E_{\text{noise}}^2 + \delta E_{\text{Poisson}}^2}$ as a dashed line. However, the results indicate that some unknown factors including the δ_{sc} make the energy resolution worse than the above relation at $>700\,\text{keV}$. When we include the constant term of intrinsic energy resolution δ_{sc} to fit the experimental result, we obtain $\delta_{\text{sc}} = 3.56 \pm 0.23\%$ which is thought to be one in the high-energy limit. For the lower gamma-rays, the electric noise of pre-amplifier determined the energy resolution, and thus reducing the electric noise is essential.

5. Readout with APD

Since we confirmed that the BGO readout with the PIN photodiode is effective at higher energy of gamma-rays, we next test the BGO + APD combination. Since we find that BGO is better than GSO for the photodiode readout, hereafter we check BGO and CsI. In Fig. 8, we show the pulse–height spectra of BGO and CsI for 662 keV gamma-ray when we read the scintillators with the APD. The spectra are remarkable; the escape line of Bi–K is clearly separated from the photo-peak in the BGO spectrum. It can be seen that the ratio of the photopeak count against the Compton tail for BGO is larger than that for CsI. The energy resolution is $6.2 \pm 0.1\%$ and $5.8 \pm 0.1\%$ for BGO and CsI. In Table 2, we summarize the energy resolution of BGO, GSO, CsI readout with PMT, PD, APD for the 662 keV gamma-ray. The value of 6.2% is better than that of the BGO + PMT, and comparable to that of CsI + PMT. In Fig. 9, we compare the energy resolution of BGO readout with PMT, PD, and APD. It can be seen that the BGO + APD is the best below 2000 keV.

We also show the BGO + APD spectrum for the ^{57}Co source in Fig. 10. The low-energy gamma-ray line of 14 keV is clearly seen, and the noise level is below 10 keV. In Fig. 11, the energy resolution obtained for various radio isotopes is plotted against the incident gamma-ray energy. The slope is around 0.5 at a wide range of 10–2000 keV, and thus apparently it seems that the poisson noise is dominant. Moszyński et al. [12] claimed that the excess noise factor F is 2–3 for their API APD, and Ikawaga et al. [5] obtained $F = 2.0$ for the APD S8664-55. Therefore, we input $F = 2$ for the formula of poisson noise and obtained $\delta E_{\text{Poisson}} = 4.13(E/662\,\text{keV})^{-0.5}\%$, which is better by a factor of 1.5 than the measured values over all the energy. When fitting the graph with the formula in Section 3 with F to be free, F becomes 4.70 ± 0.20 and δ_{sc} is constrained to be $<0.4\%$. Such a large value of F is not reasonable for the APD avalanche [13]. Following Ref. [14], we calculated the intrinsic energy resolution δ_{sc} by subtracting the contribution of $\delta E_{\text{Poisson}}$ and δE_{noise} from the measured value for PD + BGO and APD + BGO, and showed it as a function of the gamma-ray energy in Fig. 11 right. The PD + BGO gives somewhat large values of δ_{sc}, but as a whole follows the same relation as APD + BGO.

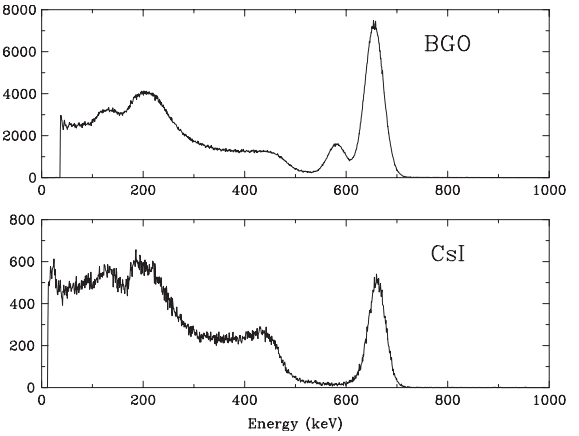

Fig. 8. Pulse–height spectra of ^{137}Cs for scintillators readout with APD; BGO (top) and CsI (bottom).

Table 2
Comparison of energy resolution (%) for the 662 keV gamma-ray

	PMT	PD	APD
BGO	7.04 ± 0.10	8.33 ± 0.28	6.24 ± 0.07
GSO	6.69 ± 0.06	9.10 ± 0.78	—
CsI	6.13 ± 0.03	6.24 ± 0.15	5.85 ± 0.11

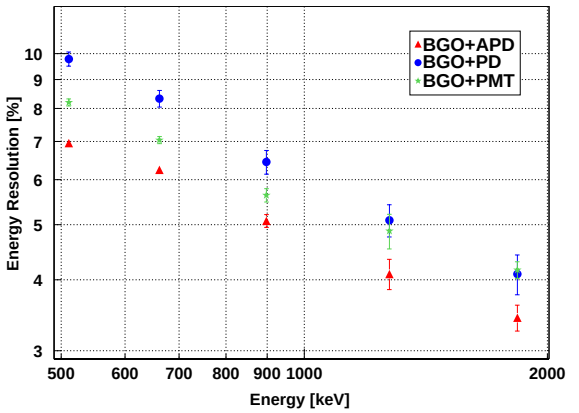

Fig. 9. Energy resolution (FWHM) of BGO readout with PMT (star), PD (circle), and APD (triangle) against the gamma-ray energy above 500 keV.

The calculated intrinsic energy resolution δ_{sc} strongly depends on the gamma-ray energy, and $4.7 \pm 0.5\%$ at 662 keV for the APD + BGO is close to $3.0 \pm 1.2\%$ of Moszyński et al. [8].

In summary, the energy resolution of BGO + APD is comparable to that of CsI + PMT at >500 keV, and limited by the some unknown mechanisms including intrinsic energy resolution of BGO.

Next, we investigated the dependence of gain on the temperature and bias voltage. The temperature dependence was measured at the bias of 290 V, and the bias dependence was measured at -30°. In Fig. 12, we show the results. It can be seen that the gain exponentially decreases as the temperature goes up, and increases with a larger slope as higher bias is supplied. The energy resolution is constant around 210–310 V. Since the threshold is inversely proportional to the gain, we chose the bias voltage of 290 V. Above 290 V, the energy resolution becomes worse, and the slope of gain-bias relation becomes steeper, and thus the avalanche fluctuation becomes large.

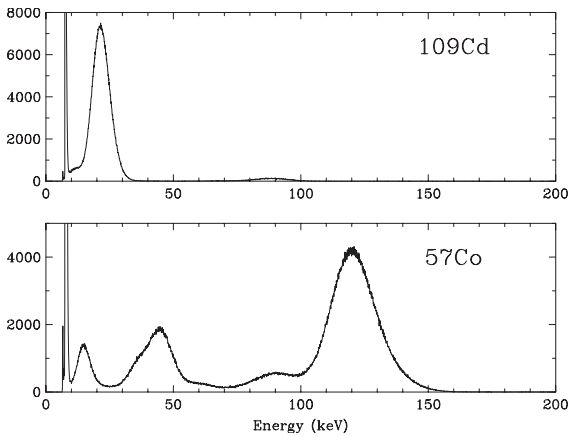

Fig. 10. Pulse–height spectra of ^{109}Cd (top) and ^{57}Co (bottom) for BGO readout with APD.

6. Stability of the APD + BGO system

For practice in the space, the APD + BGO system should be stable in the pulse–height and energy resolution for a long time. Since the APD device is novel for scintillation counters, the gain stability for a long time has not been studied. In order to test the long-term time stability, we performed the two following estimations. First of all, we tested how stable the APD + BGO is when the temperature and bias voltage is kept as constant as possible. We put the APD + BGO in the thermostatic chamber TABAI ESPEC PU-3SP to keep the temperature constant at $-30\,^{\circ}$C, supplied the bias voltage 290 V to the APD, and obtained the pulse–height spectrum at an interval of 1 h over 7 days. The temperature in the chamber was measured by the thermometer, and confirmed

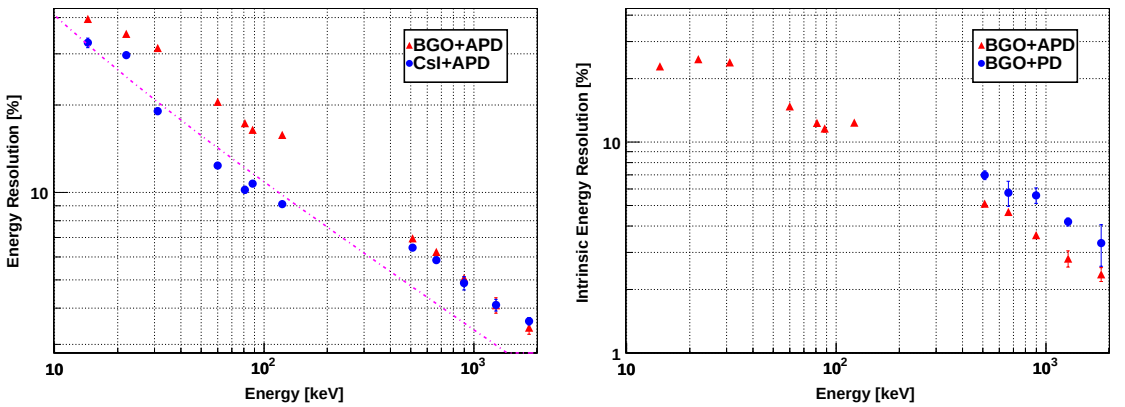

Fig. 11. (Left) Energy resolution (FWHM) of CsI and BGO readout with APD against the gamma-ray energy. The dashed line represents the predicted relation for BGO. (Right) The calculated δ_{sc} as a function of the gamma-ray energy for BGO readout with APD.

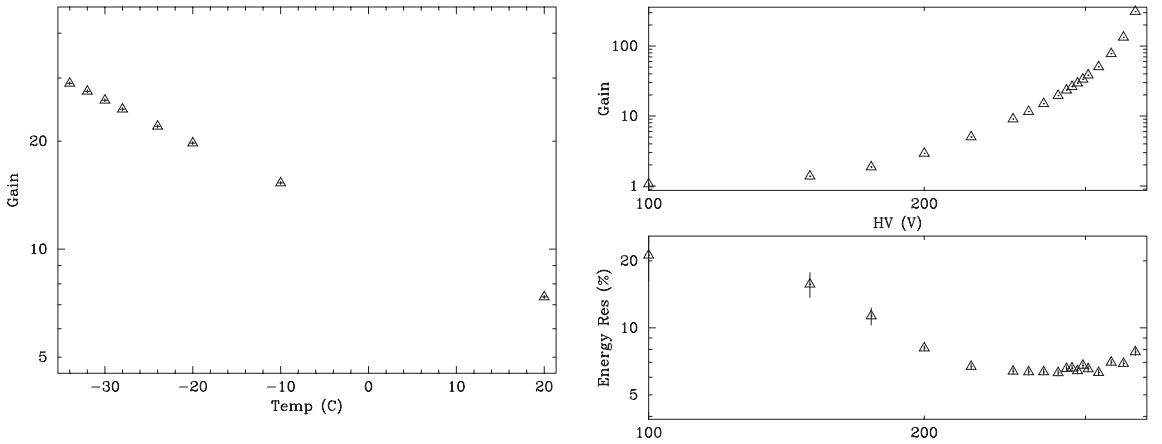

Fig. 12. The left is the temperature dependence of APD gain at $-30^{\mathrm{circ}}C$, and the right is the bias dependence of APD gain (top) and energy resolution (bottom) for the 662 keV gamma-ray.

to be stable within 1 °C. The ^{88}Y source was irradiated to the BGO. In Fig. 13, we plotted the time history of pulse–height and energy resolution of the 1836 keV photo-peak. The pulse–height slightly varies, but its amplitude is not so large; at most ±1% over 7 days. The energy resolution is also very stable within ±0.3% in the absolute value. Of course, the above variation includes the additional component due to the fluctuation of temperature and bias voltage, and thus indicates the upper limit of APD avalanche fluctuation.

In the previous section, we obtained that the pulse–height increases by −29%/°C around −30 °C as the temperature decreases, or by +2.9%/V around 290 V (gain 26) as the bias voltage increases. These are close to those of Ikagawa et al. [5] who measured around −20 °C. We must realize the gain fluctuation of <2% to keep the appropriate energy resolution. It is indicated that the requirement of fluctuation to keep the pulse–height within 2% is 0.7 °C and 0.7 V for the temperature and bias voltage, respectively. Such a temperature requirement cannot be realized in the satellite observation, although it is expected that, at least, the temperature does not vary in a short time for the detector with a large heat capacity. For the gain variation in a long time, we can trace the gain history by monitoring the background gamma-ray line accumulated in several hours. On the other hand, the requirement of bias voltage as above can be realized since such a requirement is the same level as for the PMT, which has ever been used in space.

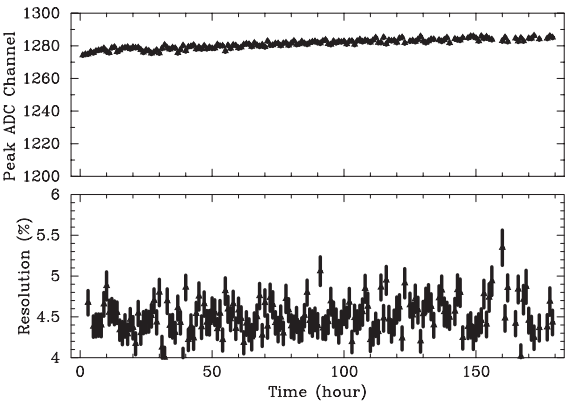

Fig. 13. Time histories of peak channel (left) and energy resolution (right) for the 1836 keV photopeak in the BGO + APD spectra at −30 °C over 7 days.

7. Conclusion and future prospect

We studied the system of the BGO readout with APD, and found that it gives an excellent performance for soft gamma-rays; a good energy resolution of 6.2% at 662 keV and <10 keV threshold energy. We also confirmed the stability of the APD + BGO system gain and energy resolution during 1 week. These suggest that the APD + BGO system is a possible good candidate

for space soft gamma-ray detector. Then, further studies must be performed, such as radiation damage, increase a sensitive area of APD, performances of APD array, readout of big BGO for the anti-coincidence detector, and so on. The radiation damage of APD was investigated and it was reported that the leakage current becomes several times larger after irradiation of neutron of 10^{12} n/cm^2 [15]. Small change of gain, temperature dependence, and quantum efficiency were also reported. Kirn et al. (1997) confirmed a 10–20% reduction of quantum efficiency after irradiation of 5.5 Mrad ^{60}Co gamma-ray [16]. Generally, the radiation damage is said to be 200rd per year, and thus the above irradiation is larger by several orders of magnitude than that in the satellite orbit.

References

[1] T. Kamae, et al., Nucl. Instr. and Meth. A 490 (2002) 456.
[2] T. Kamae, et al., SPIE 2806 (1996) 314.
[3] M. Kokubun, et al., IEEE Trans. Nucl. Sci. NS-50 (2003), in press.
[4] M. Moszyński, et al., Nucl. Instr. and Meth. A 497 (2003) 226.
[5] T. Ikagawa, et al., Nucl. Instr. and Meth. A 515 (2003) 671.
[6] M. Moszyński, et al., Nucl. Instr. and Meth. A 504 (2003) 307.
[7] T. Takahashi, et al., IEEE Trans. Nucl. Sci. NS-48 (2001) 287.
[8] M. Moszyński, et al., IEEE Trans. Nucl. Sci. NS-45 (1998) 472.
[9] M. Moszyński, et al., Nucl. Instr. and Meth. A 484 (2002) 259.
[10] M. Moszyński, et al., IEEE Trans. Nucl. Sci. NS-48 (2001) 1205.
[11] M. Moszyński, et al., IEEE Trans. Nucl. Sci. NS-44 (1997) 1052.
[12] M. Moszyński, et al., IEEE Trans. Nucl. Sci. NS-47 (2000) 1297.
[13] J.P. Pansart, Nucl. Instr. and Meth. A 387 (1997) 186.
[14] M. Moszyński, et al., IEEE Trans. Nucl. Sci. NS-46 (1999) 880.
[15] S. Baccaro, et al., CMS-NOTE-1997-030.
[16] Th. Kirn, et al., Nucl. Instr. and Meth. A 387 (1997) 202.